RESEARCH PAPER
Contrib. Sci. & Tech Eng, 2024, 1(1)
Homepage: https://cste.journals.umz.ac.ir/
DOI: 10.22080/cste.2024.5113

Contribution of Granular Platform on the Behavior of Embankment on Encased Granular Columns

Iman Hosseinpour [1]*

[1] *Associate Professor, Department of Civil Engineering, Faculty of Engineering, University of Guilan.*

Article Info
Received 14 July 2024
Accepted 16 August 2024
Available online 1 September 2024

Keywords:
Geosynthetics;
Granular Columns;
Embankment Loading;
Soft Soil;
Finite Element Analysis.

Abstract:
Conventional stone columns are widely used to improve soft soils in which high compressibility and low shear strength are observed. In very soft soils, granular columns may undergo excessive bulging due to a lack of lateral support provided by the surrounding soil. Wrapping the granular columns with appropriate geosynthetic material can reduce the total and differential settlements while improving the load-carrying capacity of the reinforced ground. A compacted sand or gravel mat (known as a working platform) placed below the embankment is commonly used to prevent excessive lateral deformation of the foundation's soft soil. In the circumstance of very high applied load, this granular mat may be further reinforced with a geogrid layer to enhance its effectiveness and control the overall stability of the embankment. This paper presents the results of a series of three-dimensional numerical analyses to study the development of hoop forces in geosynthetic encasement under different combinations of working platform thickness and basal geogrid stiffness. The results showed that for a constant working platform thickness, the hoop forces increased with the height of the embankment. The maximum values of the encasement hoop forces were also observed to reduce significantly as the thickness of the working platform increased.

***Corresponding Author:** imanhp@guilan.ac.ir

Supplementary information: Supplementary information for this article is available at https://cste.journals.umz.ac.ir/

Please cite this paper as: Hosseinpour, I. (2024). Contribution of Granular Platform on the Behavior of Embankment on Encased Granular Columns. Contributions of Science and Technology for Engineering, 1(3), 35-42. doi:10.22080/cste.2024.5113.

1. Introduction

When in-situ soft soils cannot support the desired constructions (embankments, bridges, buildings, etc), a soil improvement technique must then be adopted. Different soft soil improvement methods have been developed during the previous 50 years. Using pile/column-like elements can reduce total deformations of the improved ground and increase its bearing capacity and shear strength [1-5]. Depending on the stiffness of the stone columns, they may work similarly to piles and vertical drains. However, the strength and stiffness of a stone column depend on the external confining support provided by the surrounding soil. For very soft soils with an undrained shear strength lower than 15 kPa, conventional stone columns may not provide sufficient load-carrying capacity. Problems involved in the use of stone columns in such very soft soils include excessive bulging in the top portion and squeezing of the soft clay into the stone aggregates, affecting the permeability and performance of the system. To prevent these problems, stone columns can be encased with a suitable geosynthetic material that is capable of maintaining the drainage characteristics of the granular column, thus improving the overall column stiffness [6, 7].

Recently, numerical analysis has been successfully adopted to predict the load-bearing capacity and deformation of granular columns underlying embankments [8-10]. Based on the results of a series of numerical analyses conducted by Abusharar and Han (2011) [11], the internal friction angle, spacing, and diameter of granular columns, the shear strength and thickness of soft soil, and the internal friction angle and height of embankment fill all affected the factor of safety values against failure of the embankment. Chen et al. (2015) [12] used finite element analysis for the prediction of the behavior of a trial embankment over very soft clay stabilized with a group of encased granular columns. According to the results, geotextile encasement resulted in a higher stress concentration rate on the column's top when compared to ordinary granular columns. It was also concluded that embankment total deformations are highly associated with the stiffness of the encasement material. Ghorbani et al. (2021) [13] used finite element analysis to study the behavior of an embankment over granular columns-improved soft clay. The results of the analyses showed that when the length of the granular column was 0.75, which is the thickness of the soft clay deposit, the horizontal and vertical deformations of the embankment were reduced by about five times. Additionally, using a high-stiffness reinforcement

*ISSN **3060-6578***

underneath the embankment considerably decreased total deformations. Granular columns were also found to improve the resistance of the soft soil subjected to lateral stresses.

Based on the above discussions, using geotextile encampment can remarkably improve the performance of granular columns installed under embankments. Although the concept of encasing granular columns with geosynthetic material has previously been studied [14-20], few researchers have undertaken a study of the combined influence of the working platform and basal reinforcement on the development of hoop (radial) forces on geosynthetic encasement and tensile forces on basal reinforcement. Therefore, the current research aims to fill this gap by performing a series of fully coupled three-dimensional numerical analyses of embankment overlying a group of geotextile-encased granular columns.

2. Filed Loading Test

A test embankment on encased stone columns, located in the west of the city of Rio de Janeiro, Brazil, was considered for 3D numerical analysis. The test embankment was constructed in an area of approximately 400 m^2, in which 36 encased stone columns were installed by displacement method. The columns were 11 m in length, 0.8 m in diameter, encased by seamless woven geotextile and a center-to-center spacing between 1.75 m and 2.25 m (see Figure 1). Prior to the embankment construction, a detailed site investigation was carried out, and the geotechnical parameters of the soft clay were obtained through in situ and laboratory tests. The site investigation consisted of standard penetration tests (SPT), vane shear tests (VST), and piezocone with pore water dissipation tests (CPTu) performed at three vertical borings as reported by Hosseinpour (2015) [20]. The geotechnical profile was mainly characterized by an upper soft layer (soft clay I) extending to a depth of 7 m. Soft clay I is underlain by a thin sand lens found in a depth of 7.0 to 7.5 m. Soil profiling is followed by about 2.5 m-thick soft clay II, which is less soft, as indicated by SPT blows, and is classified as soft to medium stiff clay. The mechanical properties of geosynthetic encasement and reinforcement are shown in Table 1.

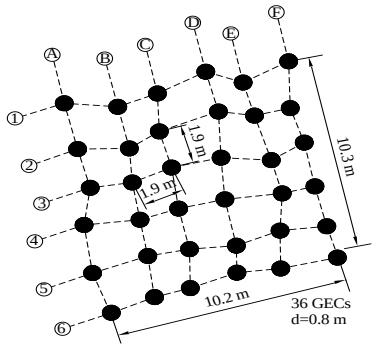

Figure 1. Schematic plan view of the GECs and overview of the test area

Table 1. Mechanical properties of geosynthetic encasement and basal reinforcement

Materials	Property	Value
Geosynthetic encasement	"Ring" tensile force (at 5% strain)	95 kN/m
	"Ring" tensile modulus (at 5% strain)	1750 kN/m
Basal reinforcement	Tensile force (at 5% strain)	82 kN/m
	Tensile modulus (at 5% strain)	2200 kN/m

The in-service performance of the test embankment over GECs composite ground was monitored to provide useful data with respect to the total vertical stresses, pore pressures, total settlements, horizontal soil displacements and column bulging. The instrumentation used for monitoring the embankment and its geometry is shown schematically in Figure 2.

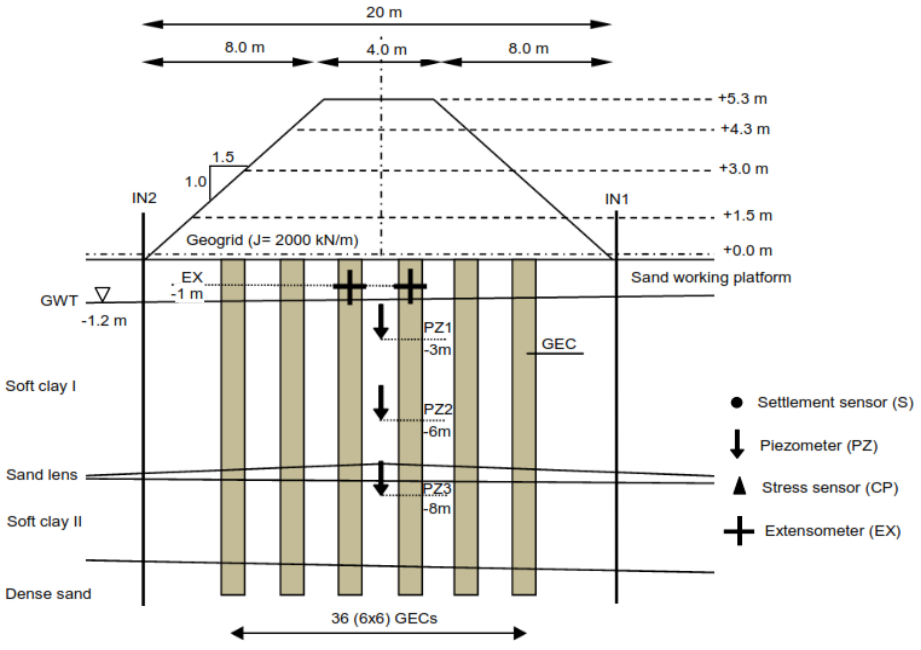

(a)

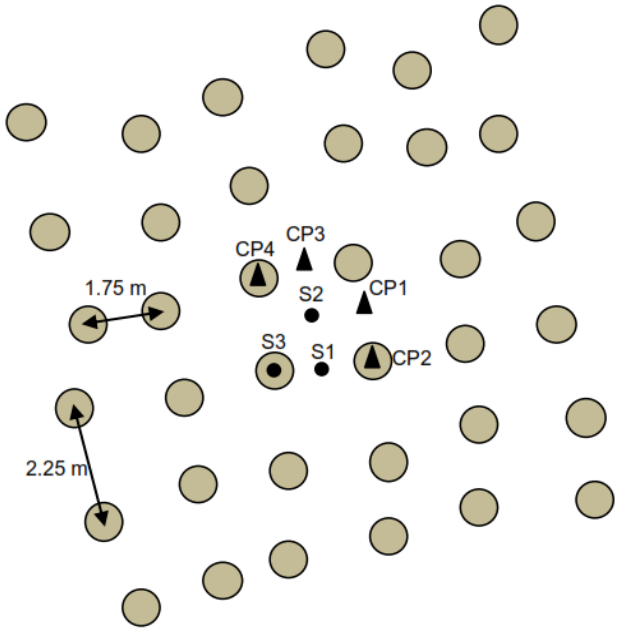

(b)

Figure 2. Filed loading test: (a) embankment side view and instrumentation layout; (b) Embankment plan view and instrumentation layout [21]

3. Finite Element Analysis

Three-dimensional numerical models were used to carry out the numerical analyses, assuming that the columns were arranged in a square pattern by an equal distance between the columns in both the longitudinal and transverse directions. The lateral extent of the model was chosen to be 40 m in order to avoid any influence of the outer boundary. No displacements in the direction perpendicular to symmetry planes were allowed; however, the model was free for vertical displacements along the lateral borders. Geosynthetic encasement and basal reinforcement were assumed to be isotropic elastic materials, implying that tensile rupture of these materials will not occur. The finite element distribution of the mesh was set to "fine" with local refinement close to the encased stone columns. The idealized geometry of the 3D model used to assess encasement hoop forces and column installation effects is shown in Figure 3.

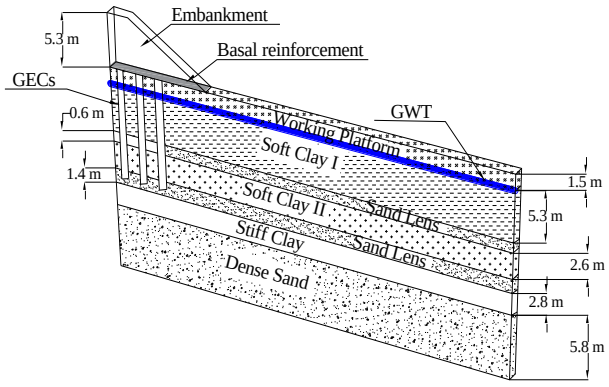

Figure 3. Three-dimensional model adopted in numerical analysis

3.1. Material Properties

Concerning the constitutive models, the elastic-perfectly plastic model with Mohr-Coulomb (MC) failure criterion was adopted for granular materials (i.e., stone column, embankment fill, sand layers, and working platform) as well as the stiff clay layer. The soft soil behavior was simulated by using a constitutive model based on the Modified Cam Clay, which is defined as soft soil (SS) in PLAXIS [21]. Geosynthetic encasement was assumed to be an isotropic elastic material with a tensile stiffness J_{enc}=1750 kN/m; this material presents a "ring" tensile force (at 5% strain) T_{ref}=95 kN/m and basal reinforcement also an isotropic elastic material with tensile stiffness J_{enc}=2200 kN/m. Tables 2 and 3, respectively, show the material properties of the granular materials, stiff clay, and soft clay layers used in numerical analyses. Those parameters were obtained from a detailed site investigation, laboratory tests, and data from well-established literature [20].

3.2. Model Validation

The three-dimensional baseline model was validated by comparing with field data from case history in terms of settlements, excess pore pressures, and geosynthetic encasement expansion with the location of the measured points shown in Figure 2. Table 4 shows the different calculation stages considered in the numerical analyses to simulate embankment construction. The first calculation step consisted of generating the initial geostatic stress state and the pore water pressures, assuming that the geosynthetic encased stone columns were previously installed. A lateral earth pressure "at-rest" condition (K_0 calculation type in PLAXIS) was adopted to define the initial stress state. In Step 1, after initial stress state generation, the option "reset displacements to zero" is chosen to avoid considering irrelevant displacements from the previous calculation step.

The following steps consisted of activating the clusters corresponding to the various embankment layers by using consolidation analysis with simultaneous loading to analyze the development and dissipation of the excess pore pressures in the saturated clay-type soil layers as a function of time. Table 4 presents a summary of the calculation steps defined in model validation.

Table 2. Parameters for granular materials and stiff clay

Material	Type	γ_{sat} (kN/m^3)	k_h (m/s)	k_v (m/s)	E´ (kN/m^2)	c´ (kN/m^2)	Ø´ (deg)	υ ' (-)	Ψ (deg)
Working platform	Mohr-Coulomb – drained	19.5	0.6	0.6	15000	0.0	33	0.3	0
Sand lens	Mohr-Coulomb – drained	18.5	0.5	0.5	22000	0.0	30	0.3	0
Embankment	Mohr-Coulomb – drained	28.0	1.0	1.0	50000	0.0	38	0.3	0
Granular column	Mohr-Coulomb – drained	20.0	10.0	10.0	80000	0.0	40	0.25	5
Dense sand	Mohr-Coulomb – drained	20.0	1.0	1.0	30000	0.0	38	0.3	0
Stiff clay	Mohr-Coulomb – drained	18.0	0.1	0.1	18000	1.0	23	0.3	0

Table 3. Parameters for soft clays

Material	Type	γ_{sat} (kN/m^3)	k_h (m/s)	k_v (m/s)	c´ (kN/m^2)	Ø´ (deg)	λ*(-)	κ*(-)
Soft Clay I	Soft soil – undrained	14.4	9.7×10^{-6}	6.2×10^{-6}	2.0	25	0.124	0.021
Soft Clay II	Soft soil – undrained	17.2	8.8×10^{-6}	5.6×10^{-6}	3.0	28	0.030	0.019

Table 4. Loading phases defined for the numerical model

Calculation step	Type of analysis	Layer thickness (m)	Total embankment height (m)	Consolidation interval (days)	Event
Initial Step	K_0 procedure	0.0	-	-	Initial stress state
Step 1	Consolidation	1.5	1.5	3	Construction
Step 2	Consolidation	1.5	1.5	10	Consolidation
Step 3	Consolidation	1.5	3.0	2	Construction
Step 4	Consolidation	1.5	3.0	32	Consolidation
Step 5	Consolidation	1.3	4.3	2	Construction
Step 6	Consolidation	1.3	4.3	14	Consolidation
Step 7	Consolidation	1.0	5.3	2	Construction
Step 8	Consolidation	1.0	5.3	180	Consolidation

Figure 4 presents the measured and calculated settlements at point S3 on the top of the encased columns (see Figure 3). As both measured and computed values show, settlement increased sharply in load application stages and then gradually increased during consolidation intervals. Accordingly, the results of numerical analyses seem to predict fairly well the measured data in both embankment construction and consolidation stages.

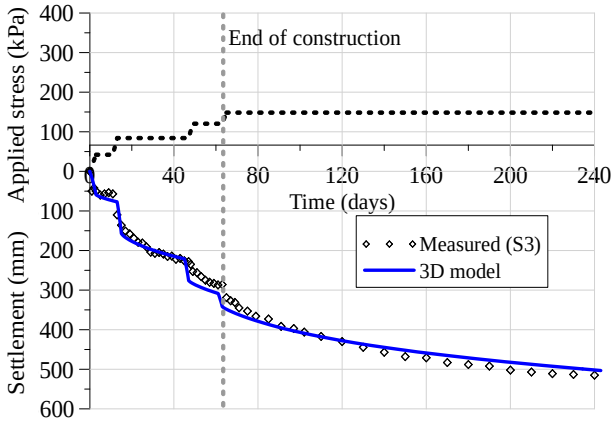

Figure 4. Computed and measured settlements at point S3

Figures 5 and 6 also show computed and measured excess pore pressures at different depths below the test embankment centerline. It can be seen that the 3D model adequately simulated the maximum excess pore pressures generated in the construction stages (i.e. peak values) and in some extent its dissipation during consolidation period. It can be concluded that the fully coupled consolidation analyses considered in the current model can adequately predict the excess pore water pressure at any depth in the soft clay layer induced by embankment loading.

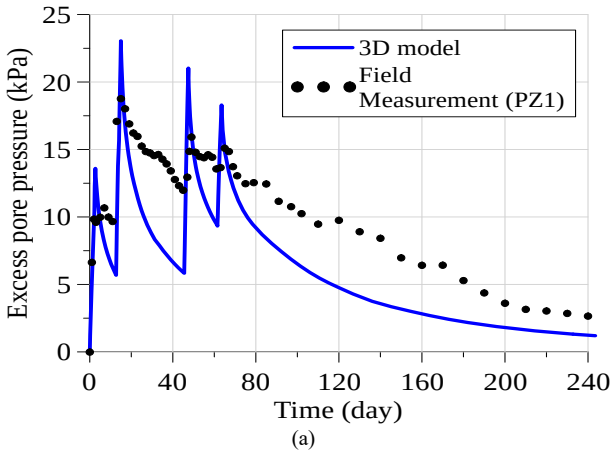

(a)

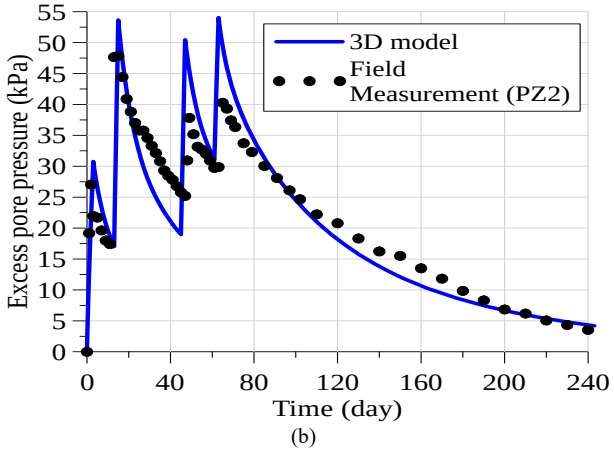

Figure 5. **Computed and measured excess pore pressures by piezometers: (a) PZ1; (b) PZ2**

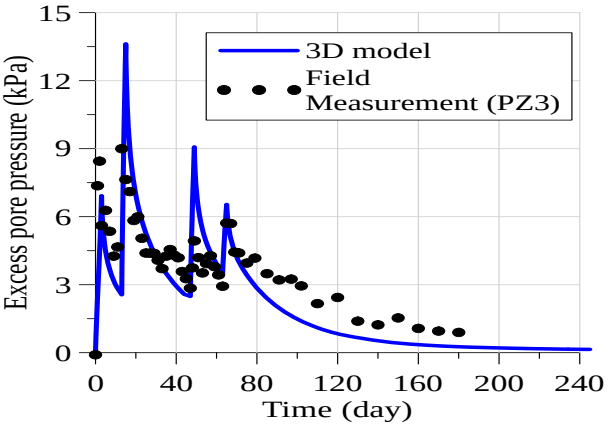

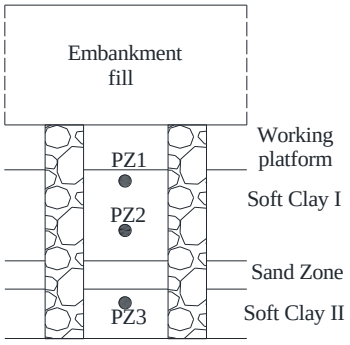

Figure 6. **Computed and measured excess pore pressures by piezometers PZ3**

Figure 7 represents the variation of measured and calculated geotextile expansions. Generally, numerical results showed good agreement in terms of the maximum geotextile expansion when compared to data measured at point D. One additional point located in the soft clay layer (i.e., point E) was selected at a depth approximately equal to the column diameter. Compared with point D, a greater geotextile expansion was observed at point E, which is attributed to the lower confining support acting on the stone column in this region.

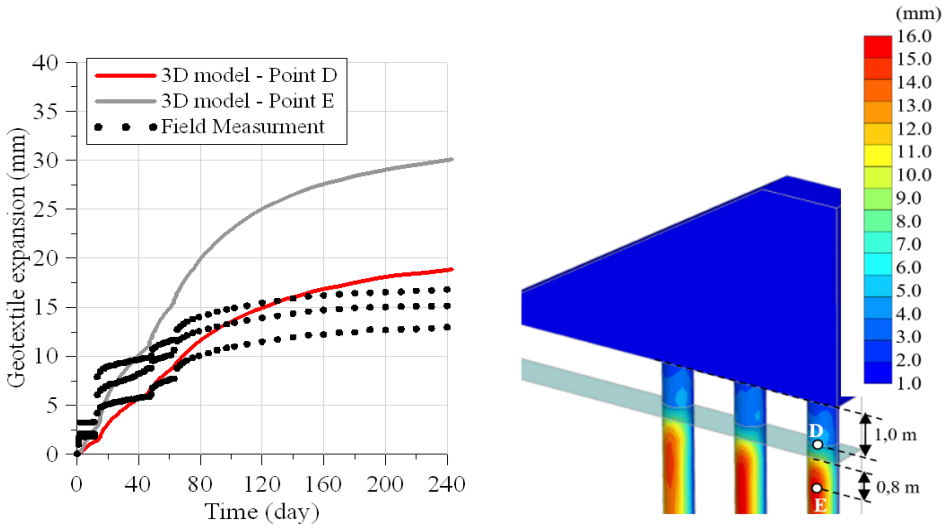

Figure 7. **Measured and computed geotextile hoop deformation**

3.3. Parametric Analyses

In this section, the variations of the maximum hoop forces developed on geosynthetic encasement and tensile forces developed on basal reinforcement for different values of working platform thickness are presented and discussed. Figure 8 shows variations in the maximum hoop force mobilized in the geosynthetic encasement for different working platform thicknesses (H_{WP}). In general, the models showed that hoop forces increased as the height of the embankment increased. For the condition without a working platform (H_{WP}=0.0 m), the maximum computed tensile forces were close to the reference tensile force of the geosynthetic encasement (T_{ref}). These values, however, reduced as the thickness of the working platform increased. It can be concluded that the relatively thick and stiff top sand layer modified the stress distribution below the embankment; subsequently, the total load transferred to the geosynthetic encased stone columns was reduced, mobilizing lower values of hoop forces developed on the geosynthetic encasement.

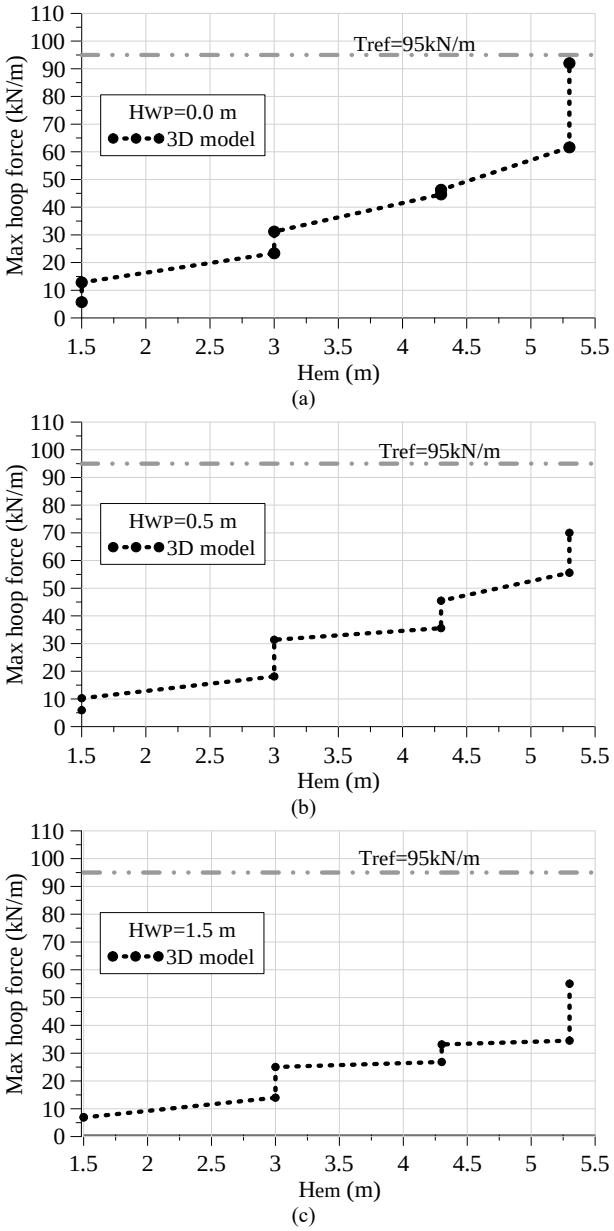

Figure 8. Computed hoop forces on geosynthetic encasement for different working platform thicknesses: (a) H_{wp}= 0; (b) H_{wp}= 0.5 m; (c) H_{wp}= 1.5 m

Figure 9 presents the maximum tensile forces that develop in the basal reinforcement as a function of the height of the embankment for different working platform thicknesses (H_{WP}=0.0 m, 0.5 m, and 1.5 m). It can be seen that reducing working platform thickness noticeably increased the tensile forces developed in basal reinforcement. For example, the maximum tensile force increased from 26 kN/m to 167 kN/m as the working platform thickness reduced from H_{WP}=1.5 m to H_{WP}=0.0 m. It should be noted that numerical analyses were performed considering the elastic behavior of the geosynthetic elements in order to compare the mobilized tensile force with the allowable tensile strength of the material (T_{ref}). From the results, the basal geogrid analyzed could be induced to failure under a condition without a working platform (H_{WP}=0.0 m) and 0.5 m-thick working platform. It can be stated that increasing working platform thickness reduces horizontal displacements below the embankment, and therefore, the amount of mobilized tensile forces of basal geosynthetic reinforcement is reduced.

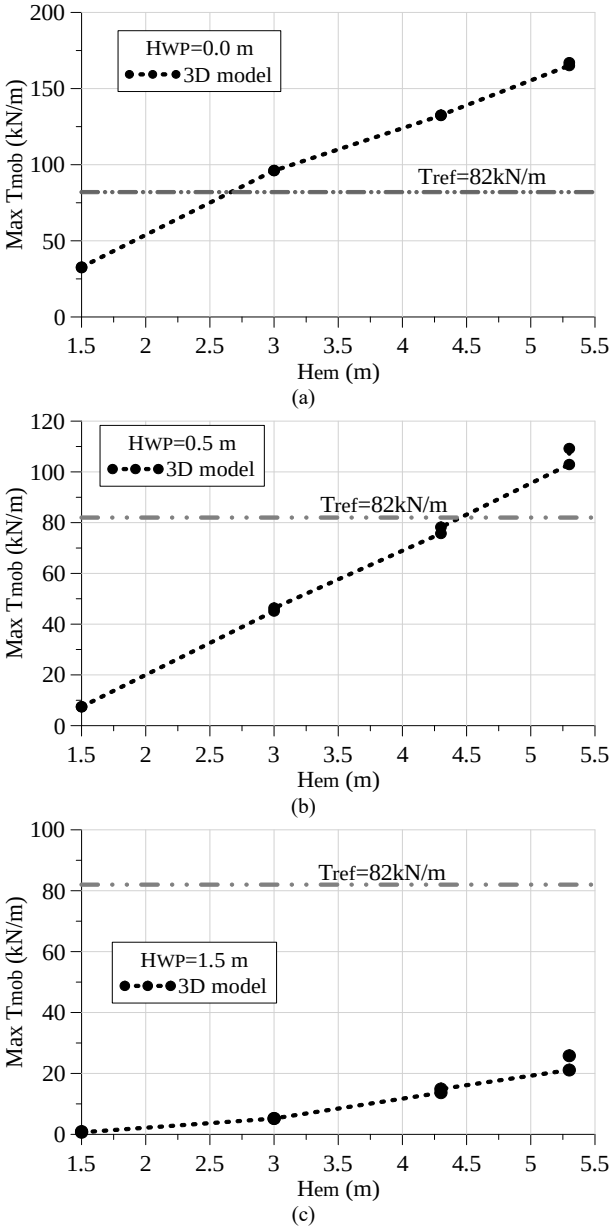

Figure 9. Computed tensile forces on basal reinforcement for different working platform thickness: (a) H_{wp}= 0; (b) H_{wp}= 0.5 m; (c) H_{wp}= 1.5 m

4. Conclusions

Following preliminary validation of a three-dimensional model with field data, this paper studies the influence of the working platform on the development of hoop forces in geosynthetic encasement and basal reinforcement in an embankment built in stages. The main results of the present study are summarized as follows:

– Results of three-dimensional models showed that increasing working platform thickness reduces the maximum hoop forces developed on geosynthetic encasement and mobilizes tensile forces on basal reinforcement. This mechanism could be associated with the stress distribution and horizontal displacement reduction below the embankment caused by the working platform, transferring a lower load to the geosynthetic

encased stone columns and reducing the mobilized tensile force of basal reinforcement. This is an important issue in terms of the design of this type of ground improvement method in order to define an optimal combination of design parameters: working platform thickness, basal reinforcement stiffness, and geosynthetic encasement stiffness.

– According to the numerical results, in the absence of a working platform, stiffer geogrid reduced maximum settlement under the embankment. The influence of the geogrid stiffness on the maximum settlement was roughly negligible as a 1.5 m-thick work platform was used. In other words, the effectiveness of the geosynthetic reinforcement was observed to be highly associated with the thickness of the working platform placed under the embankment base. This behavior was also reflected in the tension mobilized in the basal reinforcement, as the maximum value of the tensile force was greater than in other cases analyzed. In other words, the basal geogrid was responsible for a great portion of the embankment load when the working platform did not exist

5. Statements & Declarations

5.1. Acknowledgments

No acknowledgements are available for this study.

5.2. Funding

No funding resources are available for this study.

5.3. Author Contributions

Dr. Iman Hosseinpour: performing the analyses, preparing the initial and final draft.

6. References

[1] Bahadori, H., Farzalizadeh, R., Barghi, A., & Hasheminezhad, A. (2018). A comparative study between gravel and rubber drainage columns for mitigation of liquefaction hazards. Journal of Rock Mechanics and Geotechnical Engineering, 10(5), 924–934. doi:10.1016/j.jrmge.2018.03.008.

[2] Zheng, G., Yu, X., Zhou, H., Wang, S., Zhao, J., He, X., & Yang, X. (2020). Stability analysis of stone column-supported and geosynthetic-reinforced embankments on soft ground. Geotextiles and Geomembranes, 48(3), 349–356. doi:10.1016/j.geotexmem.2019.12.006.

[3] Aghili, E., Hosseinpour, I., Jamshidi Chenari, R., & Ahmadi, H. (2021). Behavior of granular column-improved clay under cyclic shear loading. Transportation Geotechnics, 31, 100654. doi:10.1016/j.trgeo.2021.100654.

[4] Alkhorshid, N. R., Araujo, G. L. S., & Palmeira, E. M. (2021). Consolidation of soft clay foundation improved by geosynthetic-reinforced granular columns: Numerical evaluation. Journal of Rock Mechanics and Geotechnical Engineering, 13(5), 1173–1181. doi:10.1016/j.jrmge.2021.03.004.

[5] Basack, S., & Nimbalkar, S. (2023). Load-Settlement Characteristics of Stone Column Reinforced Soft Marine Clay Deposit: Combined Field and Numerical Studies. Sustainability (Switzerland), 15(9). doi:10.3390/su15097457.

[6] Pandey, B. K., Rajesh, S., & Chandra, S. (2022). Time-Dependent Behavior of Embankment Resting on Soft clay Reinforced with Encased Stone Columns. Transportation Geotechnics, 36, 100809. doi:10.1016/j.trgeo.2022.100809.

[7] Hosseinpour, I., Rezvani, R., & Ebrahimzade, S. (2024). Undrained Stability Analysis of Embankment on Ordinary and Encased-Granular Columns in Soft Clay. Transportation Infrastructure Geotechnology, 11(4), 2791–2813. doi:10.1007/s40515-023-00339-6.

[8] Grizi, A., Al-Ani, W., & Wanatowski, D. (2022). Numerical Analysis of the Settlement Behavior of Soft Soil Improved with Stone Columns. Applied Sciences (Switzerland), 12(11). doi:10.3390/app12115293.

[9] Zhang, L., Peng, B., Xu, Z., & Zhou, S. (2022). Shear performance of geosynthetic-encased stone column based on 3D-DEM simulation. Computers and Geotechnics, 151, 104952. doi:10.1016/j.compgeo.2022.104952.

[10] Jasim, O. H., & Tonaroğlu, M. (2023). Using Geogrid Encased Granular Columns for Embankment's Slope Protection: 3D-Finite Difference Analysis. Applied Sciences (Switzerland), 13(4), 2448. doi:10.3390/app13042448.

[11] Abusharar, S. W., & Han, J. (2011). Two-dimensional deep-seated slope stability analysis of embankments over stone column-improved soft clay. Engineering Geology, 120(1–4), 103–110. doi:10.1016/j.enggeo.2011.04.002.

[12] Chen, J. F., Li, L. Y., Xue, J. F., & Feng, S. Z. (2015). Failure mechanism of geosynthetic-encased stone columns in soft soils under embankment. Geotextiles and Geomembranes, 43(5), 424–431. doi:10.1016/j.geotexmem.2015.04.016.

[13] Ghorbani, A., Hosseinpour, I., & Shormage, M. (2021). Deformation and Stability Analysis of Embankment over Stone Column-Strengthened Soft Ground. KSCE Journal of Civil Engineering, 25(2), 404–416. doi:10.1007/s12205-020-0349-y.

[14] Murugesan, S., & Rajagopal, K. (2006). Geosynthetic-encased stone columns: Numerical evaluation. Geotextiles and Geomembranes, 24(6), 349–358. doi:10.1016/j.geotexmem.2006.05.001.

[15] Ali, K., Shahu, J. T., & Sharma, K. G. (2014). Model tests on single and groups of stone columns with different geosynthetic reinforcement arrangement. Geosynthetics International, 21(2), 103–118. doi:10.1680/gein.14.00002.

[16] Mirrashed, A. H., Hosseinpour, I., Mirmoradi, S. H., & Ahmadi, H. (2023). Influence of Granular Columns on the Behavior of Reinforced-Soil Wall on Layered Soft Foundation. Transportation Infrastructure Geotechnology, 10(5), 749–773. doi:10.1007/s40515-022-00241-7.

[17] Fatehi, M., Yaghoobi, B., Payan, M., Hosseinpour, I., & Jamshidi Chenari, R. (2023). Combined bearing capacity of footings on geogrid-reinforced granular fill over soft clay. In Geosynthetics International. Geosynthetics International. doi:10.1680/jgein.23.00049.

[18] Mohamadi Merse, M., Hosseinpour, I., Payan, M., Jamshidi Chenari, R., & Mohapatra, S. R. (2023). Shear Strength Behavior of Soft Clay Reinforced with Ordinary and Geotextile-Encased Granular Columns. International Journal of Geosynthetics and Ground Engineering, 9(6). doi:10.1007/s40891-023-00492-5.

[19] Hosseinpour, I. (2024). Three-Dimensional Numerical Analysis of Embankment Overlying Geotextile-Encased Columns with Granular Platform. Iranian Journal of Science and Technology - Transactions of Civil Engineering, 48(3), 1641–1653. doi:10.1007/s40996-024-01390-0.

[20] Hosseinpour, I. (2015). Test embankment on geotextile encased granular columns stabilized soft ground (Doctoral dissertation, PhD Thesis, Alberto Luiz Coimbra Institute of Postgraduate Studies and Research in Engineering, Rio de Janeiro, Brazil.

[21] Brinkgreve, R. B. J., & Vermeer, P.A. (2008). PLAXIS: Finite element code for soil and rock analyses. CRC Press, , Leiden, Netherlands.